24th COBEM - 2017

24th ABCM International Congress of Mechanical Engineering
December 3-8, 2017, Curitiba, PR, Brazil

COBEM-2017-0523
FLOW UNIFORMIZATION IN PARALLEL MICROCHANNEL HEATSINK

Alan Lugarini
Admilson T. Franco
Universidade Tecnológica Federal do Paraná, Post-Graduate Program in Mechanical and Materials Engineering, Curitiba, Brazil
alanlugarinisz@yahoo.com.br
admilson@utfpr.edu.br

Abstract. *The distribution of flow through parallel microchannels is a difficult task when it comes to equating the flow rate in each branch. Flow uniformization reduces thermal stresses and increases heatsink performance. The most usual way of overcoming this problem is using inlet plenums, which consists of a large manifold area attached to the parallel microchannels, with curved or stepped outer wall. This type of manifold occupies a large space and present a challenge for compactness. In the present paper, a duct with constant cross-section is employed as manifold, and the flow distribution uniformization is achieved by varying the widths of the parallel microchannels. All channels have rectangular cross-section. The constraints of the heatsink system are the total duct volume and the area. Results show that this arrangement has relatively low nonuniformity when used with constant widths. With variable widths, the heatsink performance is slightly increased. A practical correlation is given for determining the widths distribution.*

Keywords: *microchannel heatsink, parallel microchannels, flow uniformization*

1. INTRODUCTION

As electronic systems become more compact, so must the thermal systems associated with them, such as heatsinks for example. They allow microprocessors to operate at temperature levels above which the electronic chip would lose its function. Microchannel heatsinks have been studied since Tuckerman and Pease (1981) demonstrated the high convection coefficient attained in ducts with hydraulic diameter of the order 10-6 m. There is a vast literature on parallel microchannel heat sink, especially regarding single phase flow, although flow boiling is also an appealing topic. In both cases, driving the fluid flow through the microchannels represent a challenge of its own.

If a constant cross-section duct is used as manifold and all microchannels have constant cross-section, the flow rate will be a decreasing function of microchannel position (Lee et. al., 2013). Assuming the heat flux imposed at the heat sink base is uniform, this causes a temperature non-uniformity in the heatsink. In order to overcome this situation, inlet plenum such as illustrated in Fig. 1 may be used for inducing the same flow rate in each branch. Parallel microchannels fed by inlet plenum have been studied for a wide range of applications such as microreactors (Chen et. al., 2004; Miyazaki and Maeda, 2006), micro heat exchangers (Khaled and Vafai, 2001) and micromixers (Ehrfeld et. al., 1999). This type of flow configuration occupies a large area and requires greater fluid volume, representing an obstacle to miniaturization.

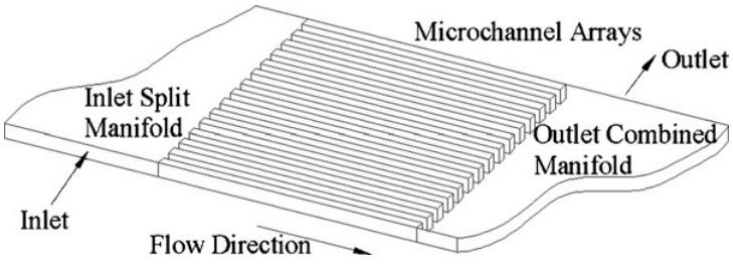

Figure 1. Representation of parallel microchannels connected to inlet and outlet plenums. Pan et. al., 2008.

Therefore, it is important to develop alternative configurations that preserve space without losing performance. Tapered channels are a possible solution, but manufacturing them in microscale is still a technical barrier (Lee et. al., 2013). In this paper we propose a simple straight duct manifold, with constant cross-section. Firstly, we analyze a configuration with constant width throughout all branches and calculate total pressure drop and flow nonuniformity. In the second part, the flow distribution uniformity is assured by varying the widths of each branch. The feasibility of each configuration is discussed.

2. CONSTANT WIDTH MODELING

The proposed flow arrangement is shown in Fig. 2. A total number of branches n is fed by a constant cross-section duct, and the flow is returned to an outlet by a duct with the same cross-section. The boundary conditions are the inlet flow rate $\dot{m}_{in}$ and the outlet pressure P_0. The branches width are w_i, where i denotes their position from the left side. All cross-sections are rectangular with constant depth (H), for ease of manufacturing and future experimental validation. The total heatsink area is L^2. The dashed line denotes an elemental volume. Each branch is responsible for cooling one of the n elemental volumes.

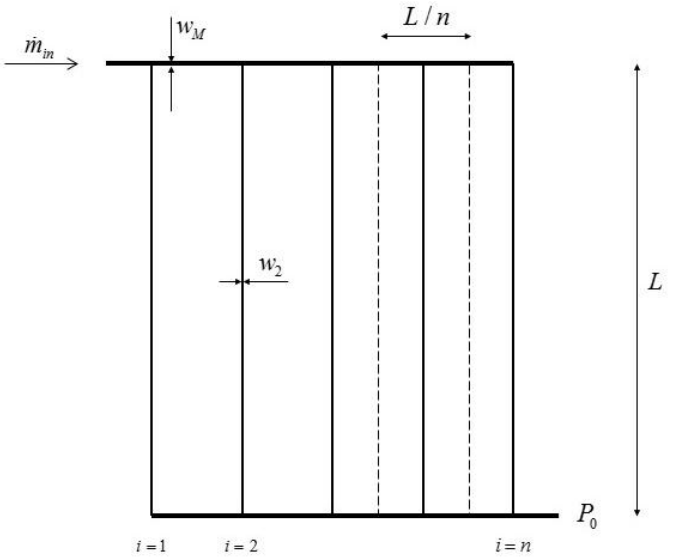

Figure 2. Flow configuration of parallel channels fed by a constant cross-section duct.

If the svelteness of the flow network is sufficiently high, the flow regime may be assumed to be laminar fully developed (Lee et. al., 2013). In such case, the pressure drop along a straight segment (ΔP) is a function of the duct's length (l) and cross-section shape and size, and the flow rate that goes through it (White, 1991):

$$\Delta P = \frac{2 f \rho V^2 l}{D_h} \tag{1}$$

where f is the Fanning friction factor, ρ is density, V is average flow velocity and D_h is the cross-section hydraulic diameter. Using the definition of Poiseuille number $Po = f\,Re$ and Reynolds number $Re = \dot{m}D_h / \nu\rho A$, one gets:

$$\Delta P = \frac{2 Po \nu \dot{m} l}{D_h^2 A} \tag{2}$$

By definition (White, 1991) $D_h = 4A / p_w = 2wH / (w + H)$, where p_w is the wetted perimeter. The Poiseuille number is a function of w only, since H is fixed. A simple and sufficient approximation is given by Bejan (2013):

$$Po = 24\left(\frac{1+\alpha^2}{1+2\alpha+\alpha^2}\right) \tag{3}$$

where α is the minimum of w / H or H / w. Assuming w << H, Eq. (2) is simplified to:

$$\Delta\tilde{P} = \frac{\Delta P}{12\nu\dot{m}/H} = \frac{l}{w^3} \tag{4}$$

The mass fraction x_i is defined as the ratio between the mass flow rate in branch i and the inlet mass flow rate. Finally, the pressure drop along a straight segment is written as a hydraulic resistance:

$$\Delta\tilde{P}_i = x_i R_i \tag{5}$$

where $R_i = l_i/w_i^3$. Considering the total fluid volume $V_f = 2(L\text{-}L/2n)w_M H + LH\sum w_i$ constant, and defining $k_i = w_i / w_M$, the hydraulic resistances of manifold channels (R_M) and branches (R_i) take the form:

$$\frac{R_M}{V_f^{-3}H^3L^4} = \frac{1}{n}\left[\left(2-n^{-1}\right)+\sum_{i=1}^{n}k_i\right]^3 \tag{6}$$

$$\frac{R_i}{V_f^{-3}H^3L^4} = \frac{1}{k_i^3}\left[\left(2-n^{-1}\right)+\sum_{i=1}^{n}k_i\right]^3 \tag{7}$$

The total pressure drop and mass fractions distribution can be determined by an electrical circuit analogy, as depicted in Fig. 3.

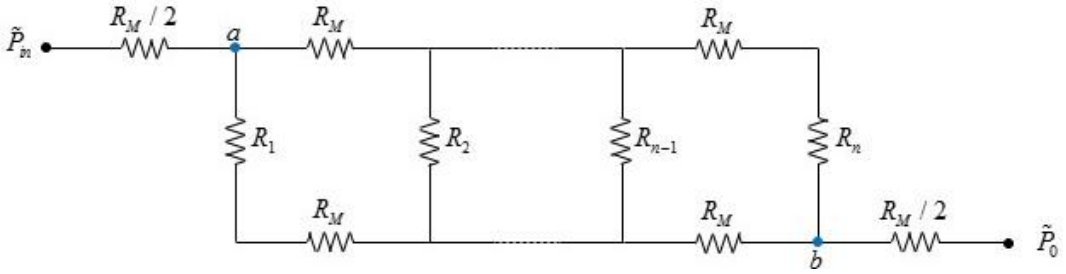

Figure 3. Electrical circuit analogy for the flow system shown in Fig. 2.

Noting that the pressure drop between point "a" and "b" must be the same over all n possible paths, the description of pressure drop have n different expressions. For an exemplary system with n = 5, the following equations are obtained:

$$\begin{cases}
\Delta\tilde{P}_{a-b} = x_1R_1 + x_1R_M + (x_1+x_2)R_M + (x_1+x_2+x_3)R_M + (x_1+x_2+x_3+x_4)R_M \\
\quad = (1-x_1)R_M + x_2R_2 + (x_1+x_2)R_M + (x_1+x_2+x_3)R_M + (x_1+x_2+x_3+x_4)R_M \\
\quad = (1-x_1)R_M + (1-x_1-x_2)R_M + x_3R_3 + (x_1+x_2+x_3)R_M + (x_1+x_2+x_3+x_4)R_M \\
\quad = (1-x_1)R_M + (1-x_1-x_2)R_M + (1-x_1-x_2-x_3)R_M + x_4R_4 + (x_1+x_2+x_3+x_4)R_M \\
\quad = (1-x_1)R_M + (1-x_1-x_2)R_M + (1-x_1-x_2-x_3)R_M + (1-x_1-x_2-x_3-x_4)R_M + x_5R_5
\end{cases} \tag{8}$$

Generalizing for the ith branch:

$$\Delta\tilde{P}_{a-b} = \sum_{j=1}^{i-1}\left(1-\sum_{k=1}^{j}x_k\right)R_M + x_iR_i + \sum_{j=i}^{n-1}\left(\sum_{k=1}^{j}x_k\right)R_M \tag{9}$$

Solving for x_i:

$$x_iR_i = x_1R_1 + \left[2\sum_{j=1}^{i-1}\sum_{k=1}^{j}x_k - (i-1)\right]R_M \tag{10}$$

where the mass fraction x_1 must be found such that the mass balance $\sum x_i = 1$ is assured. Once the mass fractions are known, the total pressure drop can be calculated by:

$$\Delta\tilde{P}_{total} = x_1 R_1 + \left(\sum_{j=1}^{n-1} \sum_{k=1}^{j} x_k + 1 \right) R_M \tag{11}$$

2.1 Mass Fraction Distribution

When all of the branches widths are the same, the geometric degrees of freedom are n and k ($k = k_1 = k_2 = \ldots$). Fig. 4 shows how the mass fractions are distributed in the case $n = 9$ for two different width ratios. The distribution in $k = 1$ indicates a less uniform flow than in $k = 0.75$. Differently from the case investigated by Lee et. al. (2013), where all branches exited to a pressure reservoir, the presence of a collector causes the minimum mass fraction to be located at the central branch. The x_i profile is parabolic in both cases.

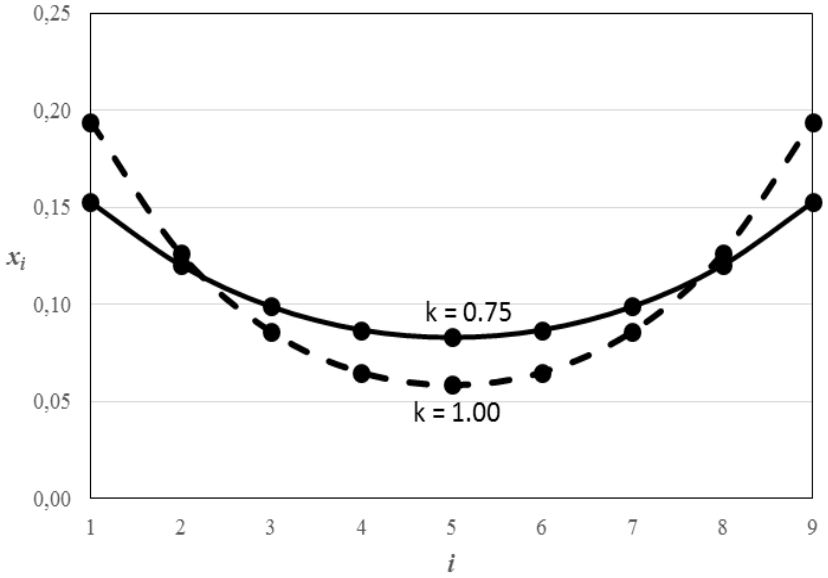

Figure 4. Mass fraction distribution for $n = 9$ and two different width ratios.

A measure of nonuniformity is necessary. Here we define a parameter μ, called flow distribution nonuniformity:

$$\mu = \frac{\bar{x}}{\min(x_i)} \tag{12}$$

where $\bar{x} = 1/n$ is the average mass fraction. The parameter μ is defined so that the total pressure drop necessary to make the least favored branch receive a mass flow rate $\bar{x}\,\dot{m}_{in}$ is $\mu\Delta\tilde{P}_{total}$. The product $\mu\Delta\tilde{P}_{total}$ is used as a goal function in the present work in the sense that the performance of the least favored branch ($i = 5$ in Fig. 4) sets the global performance for the flow system. An alternative performance evaluation method would be to consider the total pressure drop alone. The weakness of this method is the fact that it fails to represent the severity of the hot spot, which takes place exactly in the elemental volume with least mass flow rate (Lugarini, 2016).

3. VARIABLE WIDTH MODELING

It is possible to find the ideal width distribution that would provide uniform distribution over all branches. This is done by substituting x_i by $\bar{x}$ in Eq. (10). This results in:

$$R_i = R_1 - (n-i)(i-1)R_M \tag{13}$$

which implies

$$\frac{k_i}{k_1} = \left[1 - \frac{(n-i)(i-1)}{n} k_1^3 \right]^{-1/3} \tag{14}$$

valid for $k_1 < [4 / (n - 2)]^{1/3}$. The total pressure drop can still be calculated by Eq. (11). It is worth commenting that the construction rule of Eq. (14) is not an arithmetic or geometric progression. Either attempt to curve fit this rule will fail to produce ideal flow uniformity. Since for $i \geq 2$ all k_i are determined by Eq. (14), the geometric degrees of freedom in this case are n and k_1.

3.1 System Performance

The performances of both constant and variable width configurations are compared in Fig. 5. The case $n = 2$ yields $k_2 = k_1$ regardless of the configuration. The best performance point for $n = 2$ was found in $k_1 = 0.8$. This result was expected since $2^{-1/3} \approx 0.79$ is the hydraulic diameter ratio that minimizes pressure drop in bifurcations (Murray, 1926). The total pressure drop for $n = 6$ increases considerably because the actual widths of the microchannels are smaller than for $n = 2$. At $k_1 = 0.5$ the curves reach a minimum. At $k_1 = 0.7$ the maximum difference (positive) between constant and variable width configurations is reached, in which case a decrease of 5.6% is obtained for the performance parameter $\mu\Delta\tilde{P}_{total}$. For $n = 10$ the minimum is at $k_1 = 0.4$. The maximum difference (positive) between configurations is at $k_1 = 0.5$, corresponding to a 5.3% decrease in $\mu\Delta\tilde{P}_{total}$.

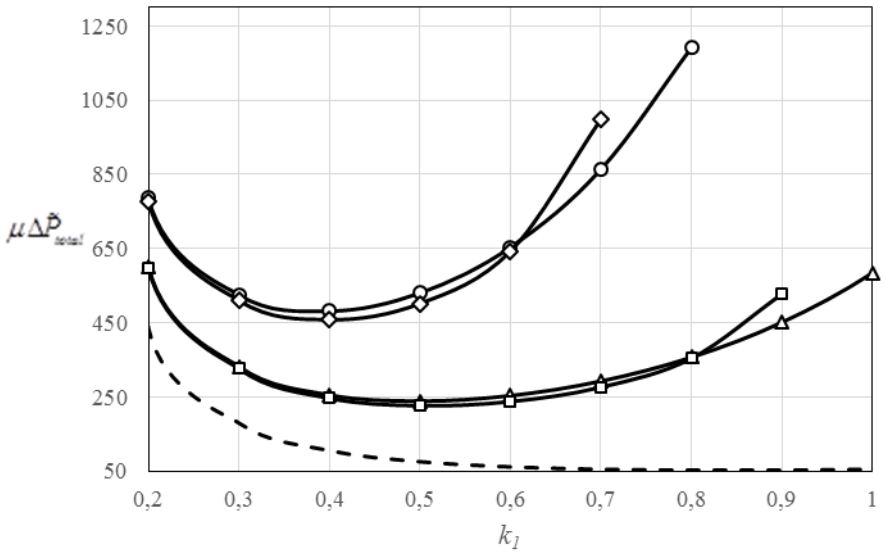

Figure 5. System performance as a function of k_1 for several configurations. Dashed line: $n = 2$. Squares: $n = 6$ (variable width). Triangles: $n = 6$ (constant width). Diamonds: $n = 10$ (variable width). Circles: $n = 10$ (constant width).

The reason performance gain obtained with variable width is so slight may be found in Fig. 6. It shows total pressure drop and flow distribution nonuniformity for a configuration with $n = 9$ and constant width. In the range of widths that correspond to the best regime, $0.3 \leq k_1 \leq 0.6$, they all provide low uniformity. The flow distribution nonuniformity μ is 1.02 for $k_1 = 0.3$ and 1.17 for $k_1 = 0.6$. Therefore, the level of uniformity provided by this configuration in this range is relatively good. The benefits of using variable width will be more evident when the manifolds resistance get higher relatively to the branches resistance. This would occur, for example, in rectangular heatsinks with branches aligned to the smaller side.

4. CONCLUSIONS

In the present work pressure drop and mass fraction distribution were solved for a network of parallel microchannels. Straight ducts were considered as manifolds, in order to reduce space occupation of inlet and outlet. Variable microchannels width was proposed with the objective of achieving flow distribution uniformization. The *status quo* was taken as a constant width configuration, which caused the central branch to receive the least mass flow rate. The implication of such nonuniformity in heatsinks is the emergence of hot spots. An electric circuit analogy was used to simplify the momentum equations. This mathematical modeling led to a construction rule for the widths ratio that promotes flow uniformity. Results showed that the variable width configuration reduces total pressure drop by approximately 5% while keeping all branches equally fed. This performance enhancement may be more important in slender devices, where the manifold length is considerably larger than the microchannels length.

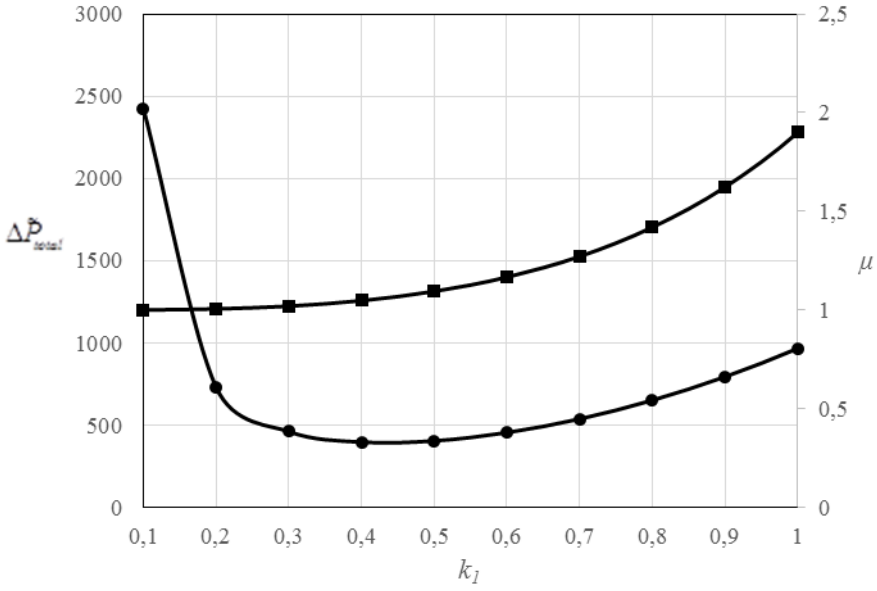

Figure 6. Total pressure drop and flow distribution nonuniformity as a function of k_1 for a configuration with $n = 9$ and constant width. Circles: $\Delta\tilde{P}_{total}$. Squares: μ.

5. REFERENCES

Bejan, A., 2013. "Convection heat transfer". 4. ed. New Jersey: John Wiley & Sons.

Chen, G., Yuan, Q., Li, H., Li, S., 2004. "CO selective oxidation in a microchannel reactor for PEM fuel cell". *Chemical Engineering Journal*, Vol. 101(1), p. 101-106.

Ehrfeld, W., Golbig, K., Hessel, V., Löwe, H., Richter, T., 1999. "Characterization of mixing in micromixers by a test reaction: single mixing units and mixer arrays". *Industrial & Engineering Chemistry Research*, Vol. 38(3), p. 1075-1082.

Khaled, A.-RA; Vafai, K., 2011. "Cooling augmentation using microchannels with rotatable separating plates". *International Journal of Heat and Mass Transfer*, Vol. 54(15), p. 3732-3739.

Lee, J., Kim, Y., Lorente, S., Bejan, A., 2013. "Constructal design of a comb-like channel network for self-healing and self-cooling". *International Journal of Heat and Mass Transfer*, Vol. 66, p. 898-905.

Lugarini, A., 2016. "Microchannel net architectures for electronics cooling". Dissertation, Federal University of Technology - Paraná, Curitiba.

Miyazaki, M., Maeda, H., 2006. "Microchannel enzyme reactors and their applications for processing". *TRENDS in Biotechnology*, Vol. 24(10), p. 463-470.

Murray, C., 1926. "The Physiological Principle of Minimum Work: I. The Vascular System and the Cost of Blood Volume". In *Proceedings of the National Academy of Sciences*, Vol. 12(3), p. 207-214.

Pan, M., Tang, Y., Pan, L., & Lu, L., 2008. "Optimal design of complex manifold geometries for uniform flow distribution between microchannels". *Chemical Engineering Journal*, Vol. 137(2), p. 339-346.

Tuckerman, D. and Pease, R., 1981. "High-performance heat sinking for VLSI". *IEEE Electron Device Lett*., Vol. 2, n. 5, p. 126-129.

White, F. M., 1991. "Viscous fluid flow". 2. ed. New York: Mcgraw-hill.

6. RESPONSIBILITY NOTICE

The authors are the only responsible for the printed material included in this paper.